Understanding Peripheral Blood Pressure Signals: A Statistical Learning Approach

Ph.D. Dissertation Defense

Md Abul Hayat

Electrical Engineering
University of Arkansas
Fayetteville, AR 72701, USA

Committee Members
Jingxian Wu, Ph.D. (Chair)
Morten O. Jensen, Ph.D.
Roy A. McCann, Ph.D.
Yue Zhao, Ph.D.

Outline

Outline

Introduction

- Peripheral Blood Pressure (PBP) Signal
  - **P**eripheral **V**enous **P**ressure (PVP) Signal
  - **P**eripheral **A**rterial **P**ressure (PAP) Signal
- The signal collection method is minimally invasive
- It can be easily collected using regular catheters
- Good representative of blood-circulation (cardiovascular) system

Outline

Motivation

- Dehydration or loss of intravascular blood volume is a common and potentially life-threatening condition
- Dehydration affects 30 million children annually and accounts for 400,000 pediatric emergency room visits in the United States.
- Up to 10% of all US hospital admissions of children <5 years of age are because of diarrhea and dehydration [WMB04]
- Assessment of fluid volume status remains an elusive problem in clinical medicine
- There is no standardized measurement for intravascular volume in adults or children
- This necessitates the development of technologies that would accurately assess the volume status of a patient to guide resuscitation and treatment

Dataset Description

- Total 18 patients of hypertrophic pyloric stenosis
- Electrolytes are used as a marker of dehydration
  - Dehydrated
    - $Cl^- < 100$ mmol/L
    - $HCO_3^- \geq 30$ mmol/L
  - Hydrated
    - $Cl^- \geq 100$ mmol/L
    - $HCO_3^- < 30$ mmol/L

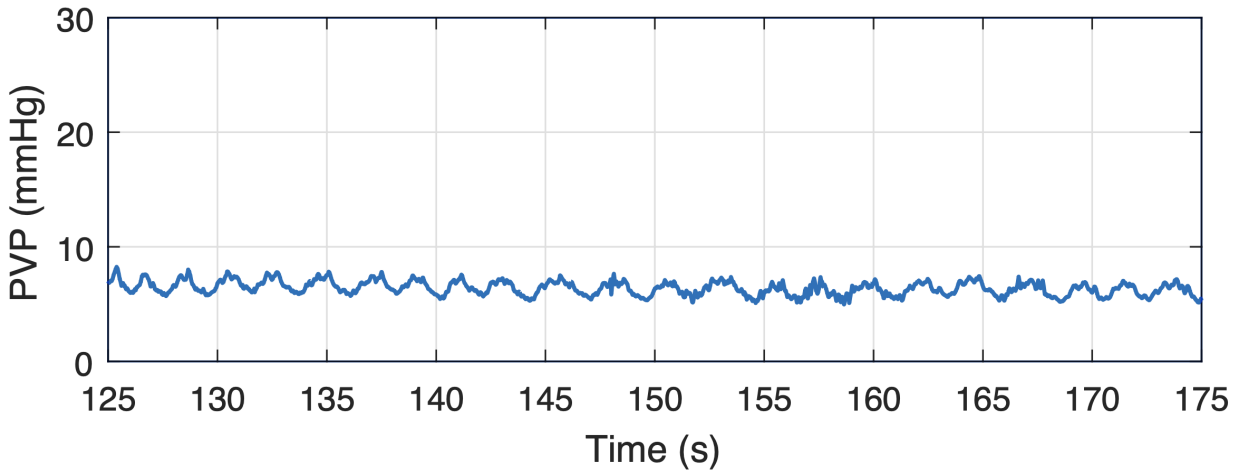

Figure 1: PVP signal

Data Acquisition System

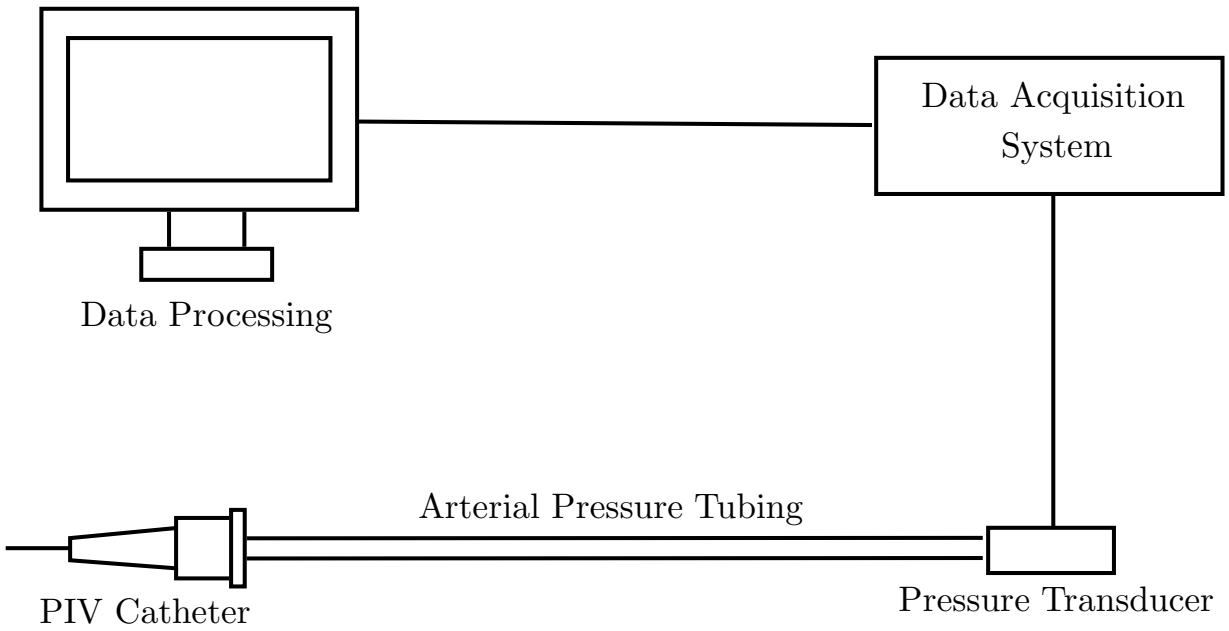

Figure 2: Schematic diagram of the data acquisition system. Peripheral intravenous (PIV) catheter is inserted into peripheral vein of a patient.

Data Pre-processing

- Splitting each patient's data into non-overlapping *windows* of 10s
- Dehydrated windows: 329
- Hydrated windows: 343
- FFT was performed over the time domain signals in each window
- Frequency domain resolution of $1/10 = 0.1$ Hz
- Each window contains 200 frequency domain samples
  - between 0 and 19.9 Hz (inclusive)
- No filtering used
- *Anomalous segments were removed manually*

Logistic Regression with Regularization

- Logistic regression is a binary classifier
- If i-th frequency domain window is X_i then

$$X_i = [1, f_0, f_{0.1}, \cdots, f_{19.9}]$$

- And corresponding label Y_i is defined as

$$Y_i = \begin{cases} 1, & \text{Dehydrated} \\ 0, & \text{Hydrated} \end{cases}$$

- This is a supervised classification problem

Classification Results

- Performance metrics
  - Sensitivity or TPR $= \frac{TP}{TP+FN}$
  - Specificity or TNR $= \frac{TN}{TN+FP}$
- Window level classification

α	Training Sensitivity(%)	Training Specificity(%)	Testing Sensitivity(%)	Testing Specificity(%)	Non-zero Coefficients
0.0001	94.40	95.87	97.94	93.07	201
0.5	99.57	99.59	96.91	93.07	73
0.75	99.57	100	96.91	92.08	64
1 (LASSO)	99.57	99.17	97.95	93.07	43

- Patient level classification
  - Majority voting on aggregate window decisions
  - Sensitivity = 100%, Specificity = 100%

Outline

Motivation

- PVP signals are highly susceptible to motion and noise artifacts
- Results presented in the previous section are based on manual removal of anomalous segments from PVP signals
- Manual removal of the anomalies introduce human bias in the result
- To remove this human bias we developed an unsupervised anomaly detection algorithm

PVP Signal Corruption

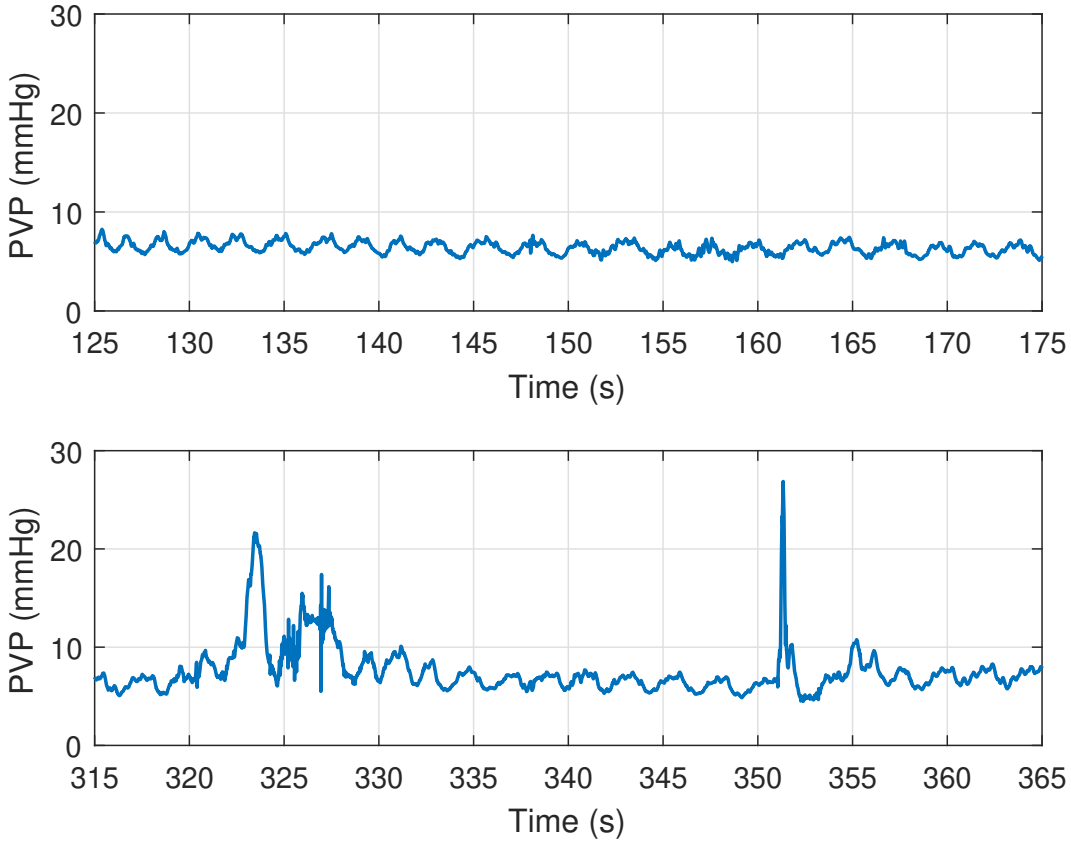

Figure 3: PVP signal (top) without anomaly and (bottom) with anomaly.

Unsupervised Anomaly Detection in PVP Signals

- To detect anomalies, we propose a two step model
- **Step-1**: PVP signals are represented and modeled using dynamic linear models (DLM)
- **Step-2**: The DLM-based Kalman filter prediction residuals are modeled using a hidden Markov model (HMM)
- DLMs are special case of *state space models* being
  - Gaussian
  - Linear and
  - Continuous

Step-1: DLM Model

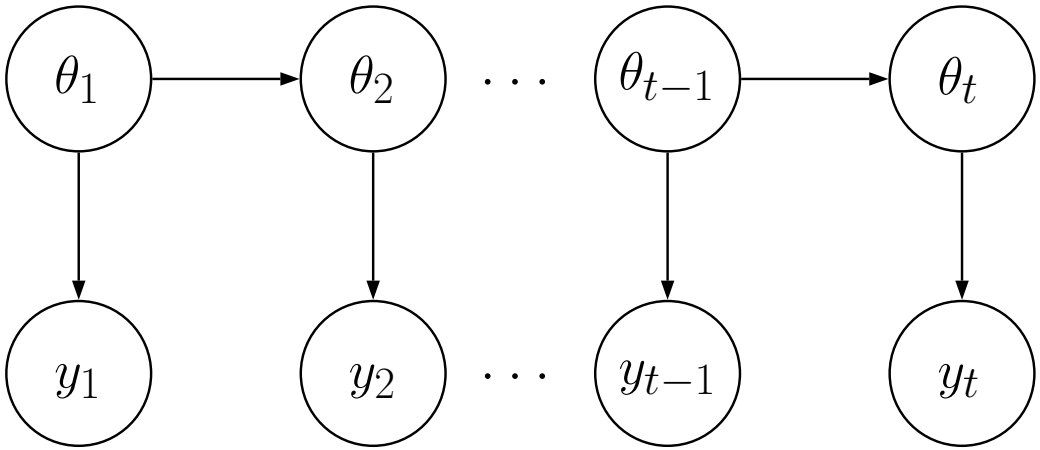

Figure 4: Dependence structure of dynamic linear model. Here, θ_i's are forming a first-order Markov chain. Also, θ_{i+1} and y_i follow a Gaussian distribution depending on θ_i under a linear relationship. $\{\theta_i\}$ and $\{y_i\}$ are continuous random variables.

Step-2: Modeling PVP Prediction Residuals with HMM

- Residual $x_t = y_t - \hat{y}_{t|t-1}$ is associated with hidden state $s_t \in \{0, 1\}$
  - $s_t = 0$ indicates normal data, and $s_t = 1$ indicates anomalies.

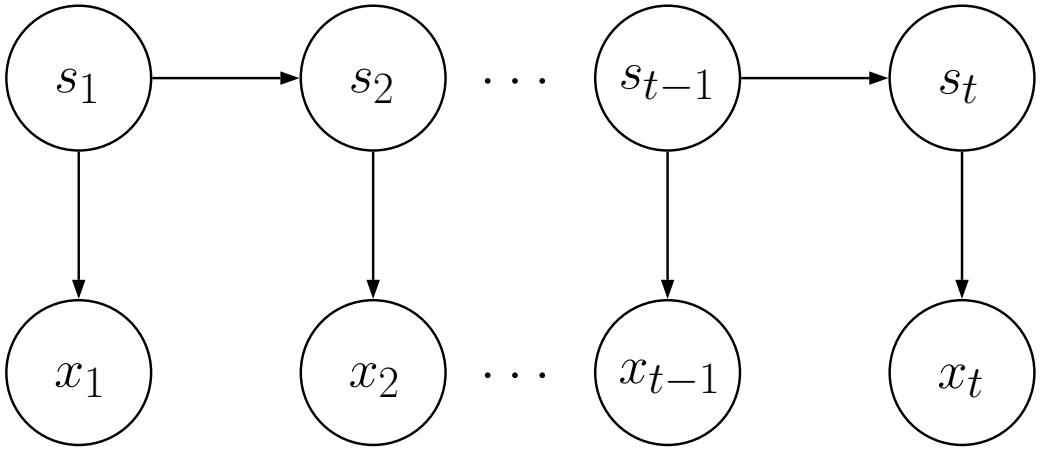

Figure 5: Dependence structure of first-order hidden Markov model. Unlike Fig. 4, here $\{s_i\}$ are discrete random variables and x_i follows a Gaussian distribution depending on s_i.

Anomaly Detection: Example

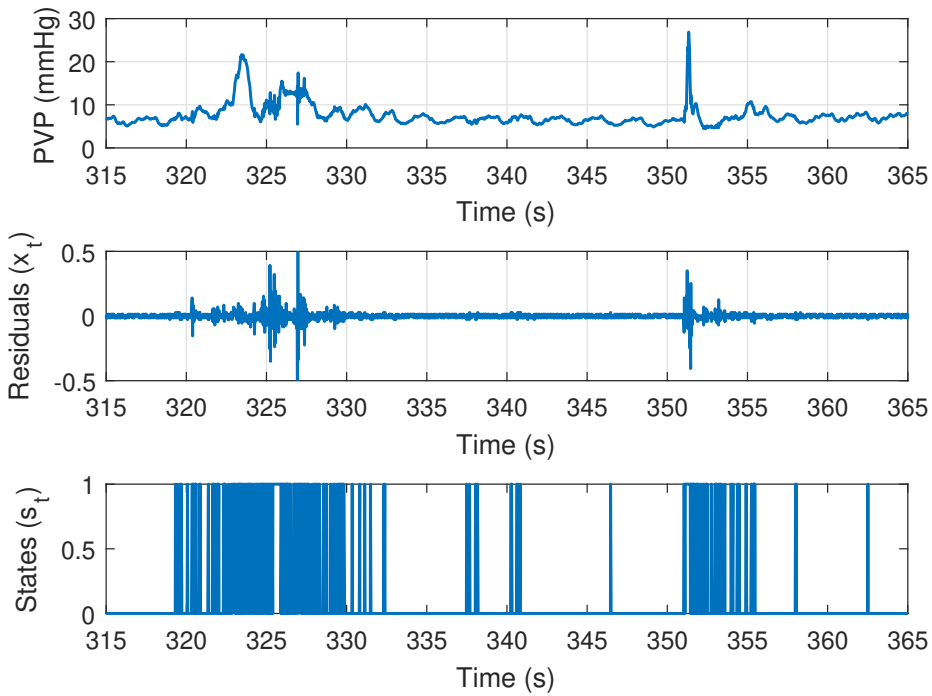

Figure 6: (Top) Anomalous PVP signal from Fig. 3; (middle) Prediction residual of the Kalman filter; and (bottom) estimated hidden states ($s_t = 0$: normal sample; $s_t = 1$: anomalous sample).

Distribution of Residuals $x(t)$

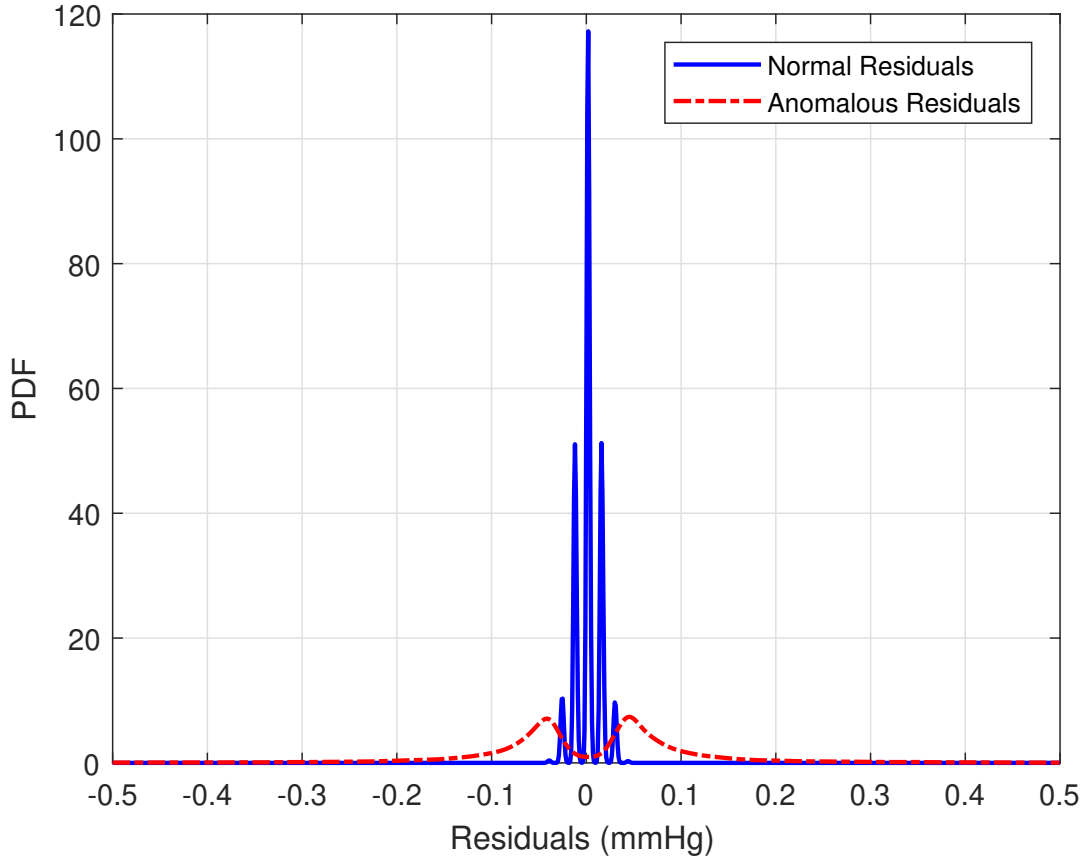

Figure 7: Empirical probability density function of residuals (x_t) from patient 10.

Normal Windows: Examples

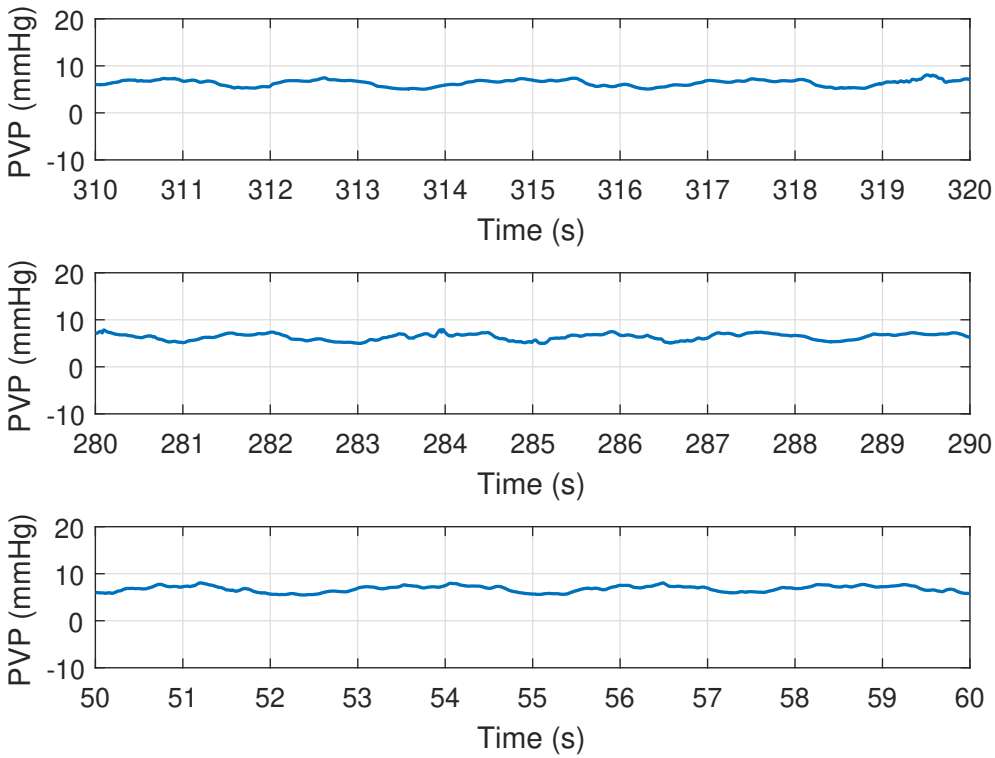

Figure 8: Example of normal windows inferred by the proposed model. Windows have a periodic structure and the amplitude does not change abruptly.

Anomalous Windows: Examples

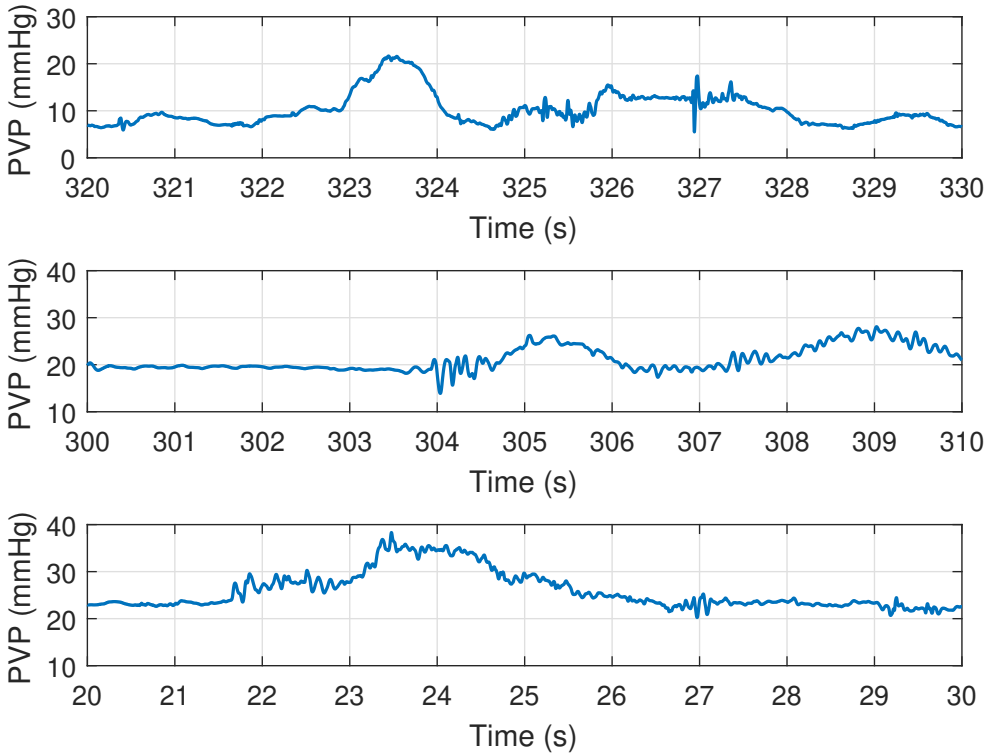

Figure 9: Example of anomalous windows inferred by the proposed model. In theses windows, amplitude changes abruptly (10-15 mmHg higher than average) indicating random motion and noise artifacts.

Classification Results

Table 1: Testing Classification Results

Parameter	Raw Data	Manual	Algorithm in [BSM+19]	Proposed Algorithm
Sensitivity	45.96%	69.35%	63.31%	71.65%
Specificity	76.08%	77.42%	79.65%	81.21%
Precision	59.68%	73.83%	71.54%	74.60%
Accuracy	62.97%	71.07%	72.35%	77.05%
Windows used	100%	70.20%	84.05%	78.92%

Outline

Motivation

- There does not exist any modeling approach for PAP and PVP signals
- A model can help us understand the interplay of different factors
- To understand the heart rate variability (HRV) in the signals
- Pig hearts have a lot of similarities with human hearts
- This is why we used pigs in this study under anesthesia

Pig Demographics

Table 2: Pig subjects used in this study

Subject	Weight (kg)	Age (weeks)	Controlled Blood Loss (ml)	Blood-Weight Ratio (ml/kg)
Pig-1	70	16	1270	18.14
Pig-2	74	17	923	12.47
Pig-3	74	17	963	13.01
Pig-4	73	17	910	12.47

Data Acquisition System

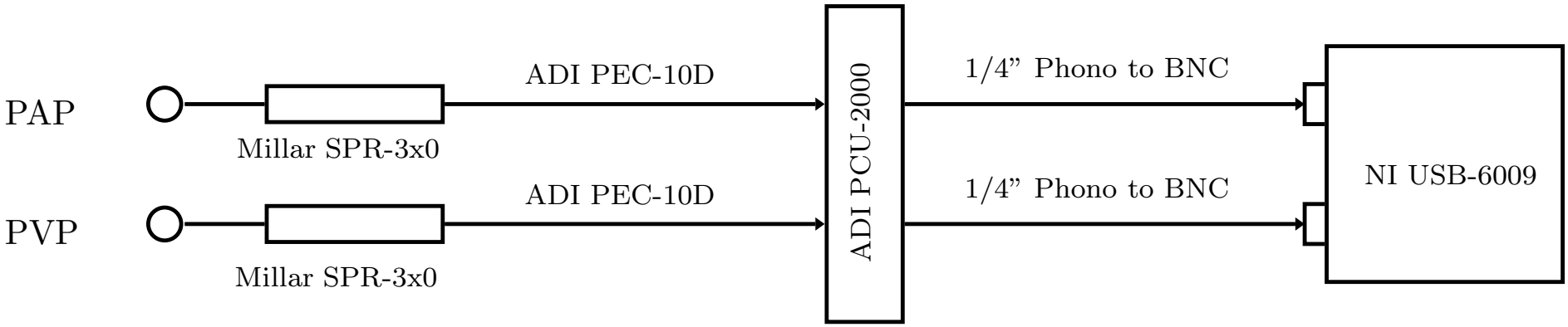

Figure 10: Schematic diagram of peripheral arterial pressure (PAP) and peripheral venous pressure (PVP) signals being collected using Millar SPR-3x0 (solid-state) catheters with National Instrument USB-6009 data acquisition system.

- We model the voltage signal recorded at the data acquisition system

Data Collection Workflow

- Two different anesthesia were used in this study
  - Isoflurane ($C_3H_2ClF_5O$) via inhalation
  - Propofol ($C_{12}H_{18}O$) injected into the veins
- Both Isoflurane and Propofol are vasodilators
  - Vasodilators widen the blood vessels
  - Vasoconstrictors constrict the blood vessels
- Increasing doses of vasodilator
  - Broadens the blood vessels
  - Similar to become hydrated from dehydration
    - Under dehydration, blood vessels constrict

Data Collection Workflow

Table 3: Asterisks (*) denote the data used in this study.

Action	Amount	Abbreviation
Isoflurane (%)	*1.80	MAC-1
	*2.50	MAC-2
	*2.80	MAC-3
	2.00	
	1.50	
Propofol (mg/kg/min)	*0.10	PRO-1
	*0.15	PRO-2
	*0.20	PRO-3
	0.05	
Bleeding		
Propofol	0.05	
Isoflurane	1.50	
	2.00	

PAP and PVP Signals

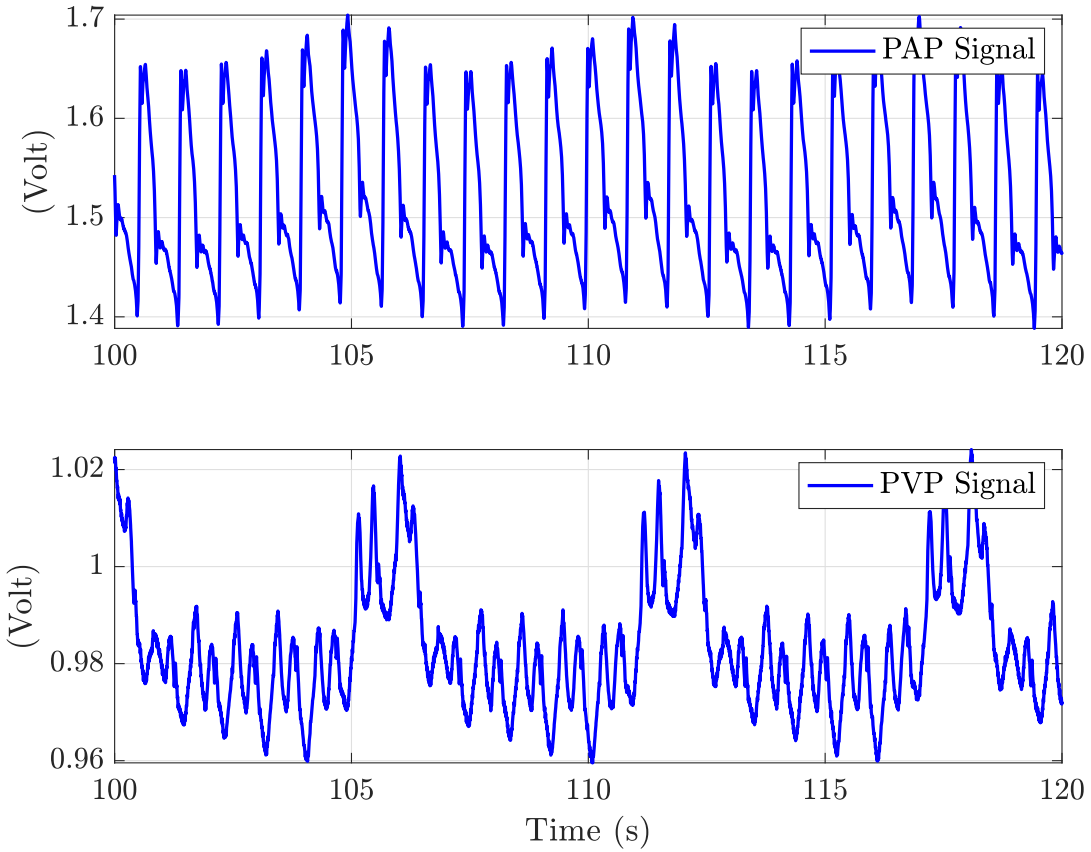

Figure 11: Example of PAP (top) and PVP signals (bottom) from Pig-2 MAC-2.

Heart Rate Variability

- The heart rate does not remain constant over time
- The variation in heart rate is called heart rate variability (HRV)
- High HRV indicates a healthy nervous system
- HRV can be contributed by multiple sources
- The main cause of HRV is respiration
- Heart rate increases and decreases with inhalation and exhalation
- Respiratory-induced HRV is called respiratory sinus arrhythmia (RSA)
- There are also other long-term sources of HRV such as
  - Autonomic nervous system imbalance
  - Heart diseases (like Arrhythmia)
  - Stress, poor sleep, unhealthy diet, and lack of exercise, etc

Parametric Signal Modeling

The IPFM-based parametric model is based the following assumptions

- Pulse onsets are initiated by modulating signal $m(t)$
- Impulse is generated if integration of $m(t)$ reaches a certain threshold
- $m(t)$ is a zero-mean signal and $|m(t)| \ll 1$
- Fourier transform $\mathscr{F}\{m(t)\} = M(\omega)$ is bandlimited
- Negligible power spectral density beyond 0.4-0.5 Hz [ML00; LS04]

Parametric Signal Modeling

If t_k as the pulse onset time of the k-th heartbeat. The following equation relates t_k with $m(t)$ [ML00, Equation (1)]

$$T = \int_{t_k}^{t_{k+1}} [1 + m(t)]dt, \tag{1}$$

or alternatively

$$k = \int_{0}^{t_k} \frac{1 + m(t)}{T} dt, \tag{2}$$

where T is the mean heart rate interval in seconds, and $\frac{1}{T}$ is the mean heart rate in Hertz and $k \in \mathbb{Z}^+$.

Parametric Signal Modeling

Another signal is the heart timing signal $\theta(t_k)$, which is defined as

$$\theta(t_k) = kT - t_k = \int_0^{t_k} m(\tau)d\tau. \tag{3}$$

The knowledge of $\theta(t)$ can be used to estimate the signal $m(t)$ as

$$m(t) = \frac{d\theta(t)}{dt}. \tag{4}$$

Parametric Signal Modeling

If the heart rate signal is $x(t)$ and heartbeat pulse is $p(t)$ with support T. Then

$$x(t) = \sum_k p\left(\frac{T}{t_{k+1} - t_k} t\right) \otimes \delta(t - t_k), \tag{5}$$

(5) can be simplified to

$$x(t) = p(t) \otimes \sum_k \delta(t - t_k). \tag{6}$$

This approximation is only used to facilitate the modeling process. The final modeled signal still follows (5).

Parametric Signal Modeling

Once the pulse onset time instants $\{t_k\}_{k\in\mathbb{Z}^+}$ are known, a non-uniformly spaced pulse train is defined as

$$s(t) \triangleq \sum_k \delta(t - t_k), \tag{7}$$

$$= \frac{1 + m(t)}{T}\left[1 + 2\sum_{n=1}^{\infty}\cos\left(\frac{2n\pi}{T}\left(t + \theta(t)\right)\right)\right]. \tag{8}$$

Thus,

$$x(t) = p(t) \otimes \sum_k \delta(t - t_k) = p(t) \otimes s(t).$$

Parametric Signal Modeling

Using the definitions, the observed PAP or PVP signal $y(t)$ is modeled as

$$y(t) = \tau(t) + \big[\alpha + r(t)\big]\big[\beta + x(t)\big]. \tag{9}$$

Here,

- $\tau(t)$ is a slow-changing bias or drift with zero mean
- $r(t)$ is the zero-mean respiratory signal
- $x(t) = p(t) \otimes s(t)$ is the heart rate signal
- α and β are the DC offsets of $r(t)$ and $x(t)$, respectively

Model Reformulation

We apply reformulation will facilitate the model estimation process.

$$h(t) \triangleq 2\sum_{n=1}^{\infty} \cos\left(\frac{2n\pi}{T}\left(t+\theta(t)\right)\right)$$

$$\gamma \triangleq \frac{1}{T}\int_{0}^{T} p(t)dt,$$

$$q(t) \triangleq \frac{1}{T}p(t) \otimes \left[m(t)(1+h(t))\right].$$

Model Reformulation

Combining

$$y(t) = \tau(t) + y_{\text{LF}}(t) + y_{\text{HF}}(t), \tag{10}$$

where

$$y_{\text{LF}}(t) \triangleq \big[\beta + \gamma\big]\big[\alpha + r(t)\big], \tag{11}$$

$$y_{\text{HF}}(t) \triangleq [\alpha + r(t)]\tilde{x}(t). \tag{12}$$

Here, $\tilde{x}(t) \triangleq x(t) - \gamma$.

Model Fitting

- Step-1: Band-limiting the input signal $y_r(t)$ to discard frequency components beyond 15 Hz and this filtered signal is denoted as $y(t)$.
- Step-2: Apply a simple moving average filter with a window length of 30 s to extract the zero-mean bias $\tau(t)$ of the signal.
- Step-3: Apply a low-pass filter with cutoff frequency $f_0 = 0.5$ Hz to the bias-corrected signal, $\tilde{y}(t) = y(t) - \tau(t)$, to separate low and high frequency component $y_{\text{LF}}(t)$ and $y_{\text{HF}}(t)$ respectively as

$$\tilde{y}(t) = y(t) - \hat{\tau}(t) = y_{\text{LF}}(t) + y_{\text{HF}}(t).$$

Model Fitting

- Step-4: Find the upper and lower envelope $e_u(t)$ and $e_l(t)$ respectively of the signal $y_{\text{HF}}(t)$.
- Step-5: Estimate α, $\beta+\gamma$, $r(t)$ and $\tilde{x}(t)$ using the following equations

$$\alpha = \frac{\bar{e}_u - \bar{e}_l}{2},$$

$$\beta + \gamma = \frac{\bar{y}_{\text{LF}}}{\alpha},$$

$$r(t) = \frac{y_{\text{LF}}(t)}{\beta+\gamma} - \alpha,$$

$$\tilde{x}(t) = \frac{y_{\text{HF}}(t)}{\alpha + r(t)}.$$

Model Fitting

- Step-6: The signal $\tilde{x}(t)$ is used to estimate $\{t_k\}_{k\in\mathbb{Z}^+}$ or $s(t)$, $p(t)$ and T using onset detection algorithm. Pulse $p(t)$ is used to estimate γ as

$$\gamma = \int_0^T p(t)dt.$$

- Step-7: To incorporate pulse width modulation, using (5)

$$\hat{x}(t) = \sum_k p\left(\frac{T}{t_{k+1}-t_k}t\right) \otimes \delta(t-t_k).$$

- Step-8: Synthesize $\hat{y}(t)$ as follows

$$\begin{aligned} y_{\text{LF}}(t) &= \big[\beta+\gamma\big]\big[\alpha+r(t)\big] \\ y_{\text{HF}}(t) &= \big[\alpha+r(t)\big]\big[\hat{x}(t)-\gamma\big] \\ \hat{y}(t) &= \tau(t)+y_{\text{LF}}(t)+y_{\text{HF}}(t) \end{aligned}$$

PVP Pulse Onset Detection

- Pulse onset is detected using finding peaks of inverted signal $-\tilde{x}(t)$
- Wait for a certain time after detecting a peak
- Wait time depends on the fundamental frequency of heart rate signal
- Wait time is in the range between 500-800 ms
- Using "findpeaks()" function of Matlab

PAP Pulse Onset Detection

- Onset detection is performed on Slope sum function (SSF) [ZHMM03]
- This SSF is basically the accumulation of non-zero slopes looking back in time over a certain duration
- The SSF signal has a sharp rise after the systolic onset
- Once onset is found, pause for the next 500 ms

Model Fitting: Step-1 & 2

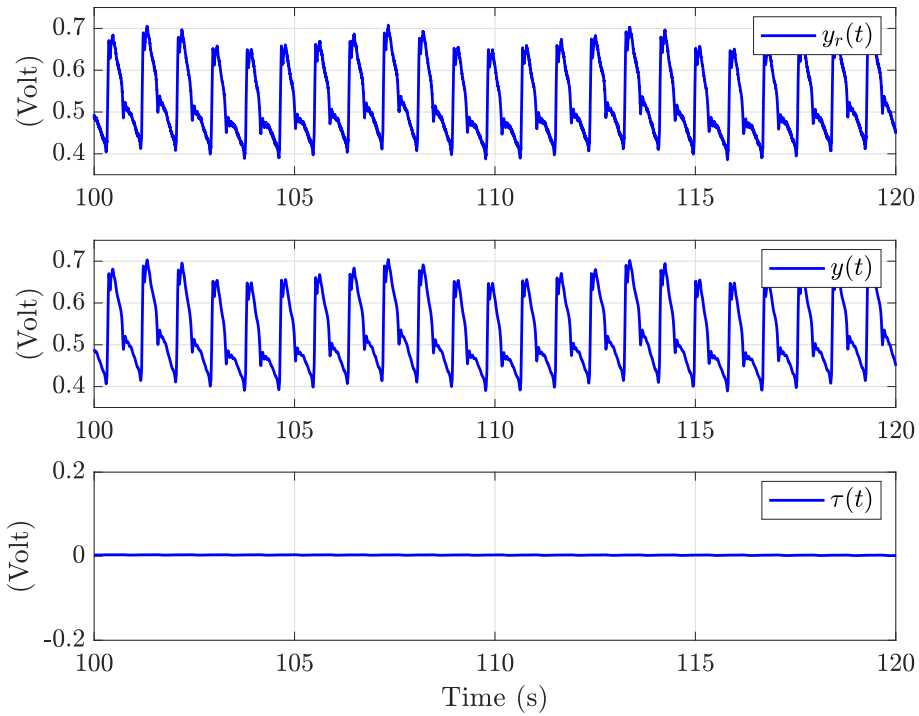

Figure 12: Example of separating high-frequency noise and trend from recorded signal $y_r(t)$ (Pig-2 MAC-2 PAP). Here, $y(t)$ obtained after filtering $y_r(t)$ and $\tau(t)$ is zero-mean trend of the signal $y(t)$. Regarding $\tau(t)$, the whole signal recording has a mean zero.

Model Fitting: Step-3

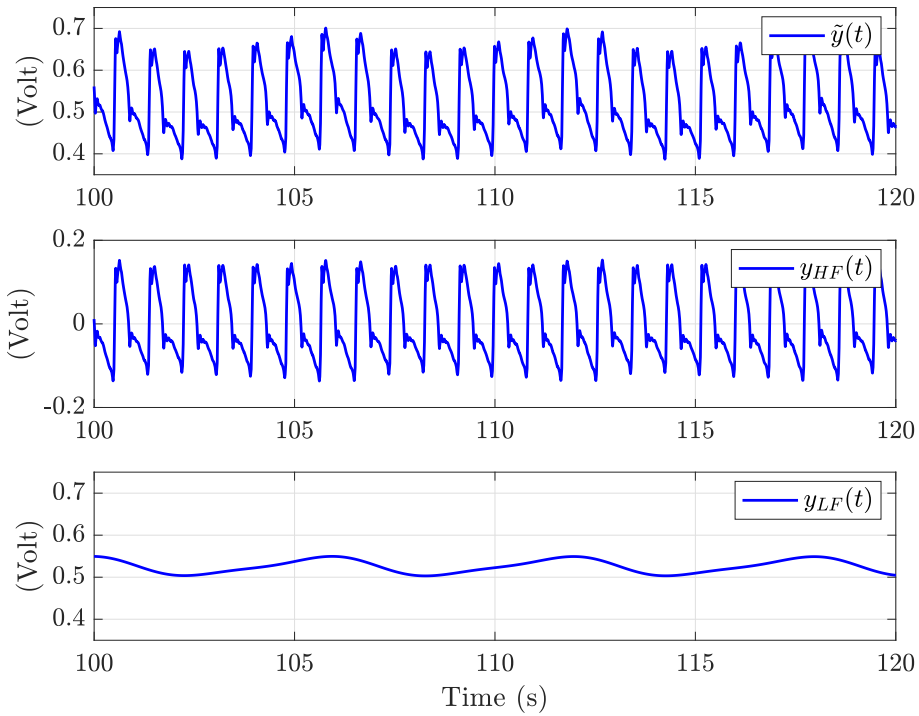

Figure 13: Separating high-frequency component $y_{\text{HF}}(t)$ and low-frequency component $y_{\text{LF}}(t)$ from $\tilde{y}(t) = y(t) - \tau(t)$ signal (Pig-2 MAC-2 PAP). $y_{\text{LF}}(t)$ is a linear transformation of respiratory signal $r(t)$.

Model Fitting: Step-4 & 5

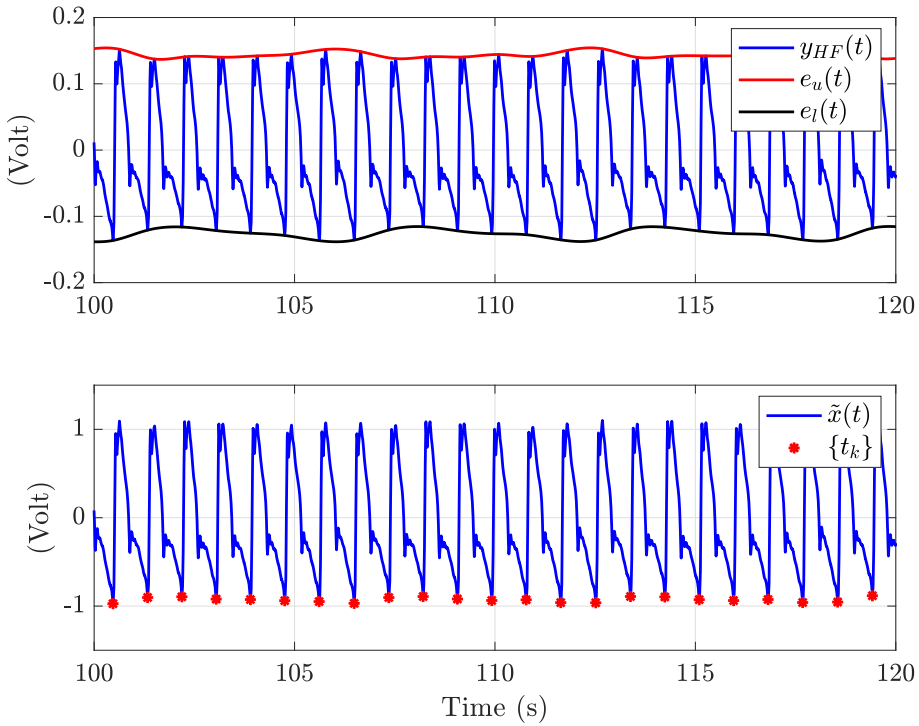

Figure 14: Estimating envelope $e_u(t)$ and $e_l(t)$ from $y_{\text{HF}}(t)$ signal (Pig-2 MAC-2 PAP). The model aims to flatten the envelope for $\hat{x}(t)$ signal.

Model Fitting: PAP Signal

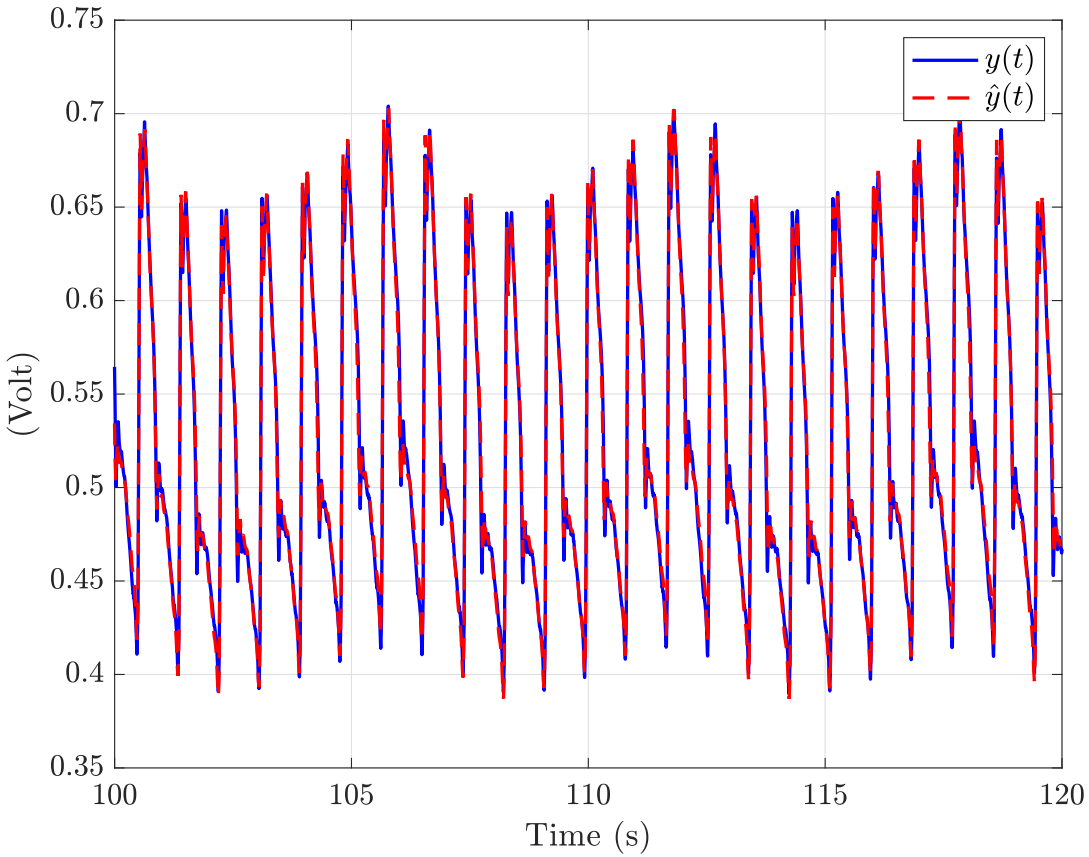

Figure 15: The PAP signal $y(t)$ and corresponding synthesized signal $\hat{y}(t)$ from Pig-2 MAC-2 with $\rho = 0.997$.

Model Fitting: PVP Signal

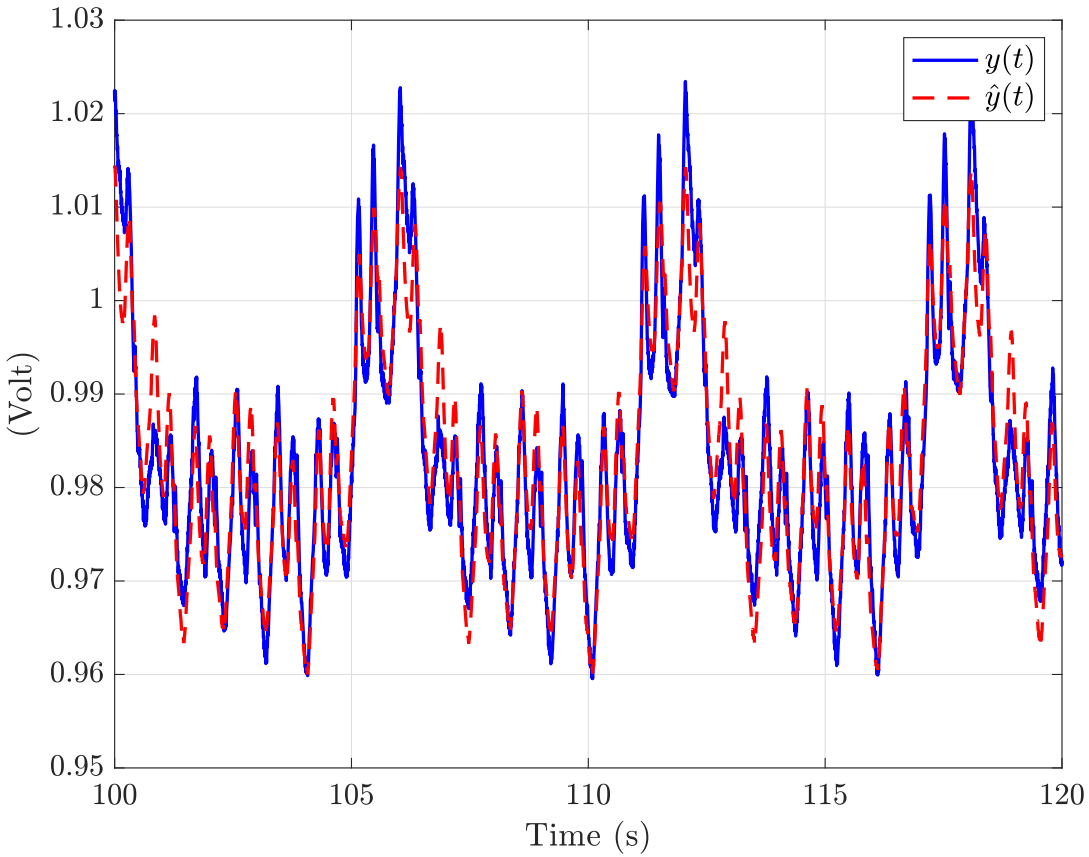

Figure 16: The PVP signal $y(t)$ and corresponding synthesized signal $\hat{y}(t)$ for Pig-2 MAC-2 with $\rho = 0.904$.

Dataset Description

- The PAP and PVP signals are synchronized and have same duration
- The sampling rate of all the signals is 1,000 samples/s

Table 4: PAP and PVP Signal duration (unit: minutes).

Subject	MAC-1	MAC-2	MAC-3	PRO-1	PRO-2	PRO-3
Pig-1	21.08	13.79	2.42	20.58	16.94	9.89
Pig-2	18.74	6.45	22.30	20.01	12.50	13.31
Pig-3	20.84	20.37	19.89	33.43	19.43	30.38
Pig-4	20.12	19.97	10.00	20.39	21.34	20.39

Model Fitting Performance

To evaluate the similarity between the experimental and model-synthesized signals, Pearson's correlation coefficient has been used.

$$\rho = \frac{\sum_i (y[i] - \bar{y})(\hat{y}[i] - \bar{\hat{y}})}{\sqrt{\sum_i (y[i] - \bar{y})^2} \sqrt{\sum_i (\hat{y}[i] - \bar{\hat{y}})^2}}. \tag{13}$$

Here, $y[n]$ and $\hat{y}[n]$ are discrete time samples of the signal $y(t)$ and $\hat{y}(t)$, respectively. Also, $\bar{y}$ and $\bar{\hat{y}}$ are the mean of the samples $y[n]$ and $\hat{y}[n]$.

Model Fitting Performance

Table 5: Correlation coefficient ρ for the IPFM model in PAP signal.

Subject	MAC-1	MAC-2	MAC-3	PRO-1	PRO-2	PRO-3
Pig-1	0.994	0.992	0.992	0.995	0.995	0.995
Pig-2	0.996	0.997	0.997	0.992	0.995	0.994
Pig-3	0.999	0.999	0.998	0.995	0.992	0.996
Pig-4	0.998	0.997	0.993	0.983	0.996	0.997

Model Fitting Performance

Table 6: Correlation coefficient ρ for the IPFM model in PVP signal.

Subject	MAC-1	MAC-2	MAC-3	PRO-1	PRO-2	PRO-3
Pig-1	0.930	0.927	0.784	0.922	0.912	0.905
Pig-2	0.921	0.904	0.913	0.952	0.954	0.941
Pig-3	0.952	0.959	0.952	0.947	0.957	0.940
Pig-4	0.902	0.884	0.828	0.905	0.871	0.879

MAC and PRO Classification

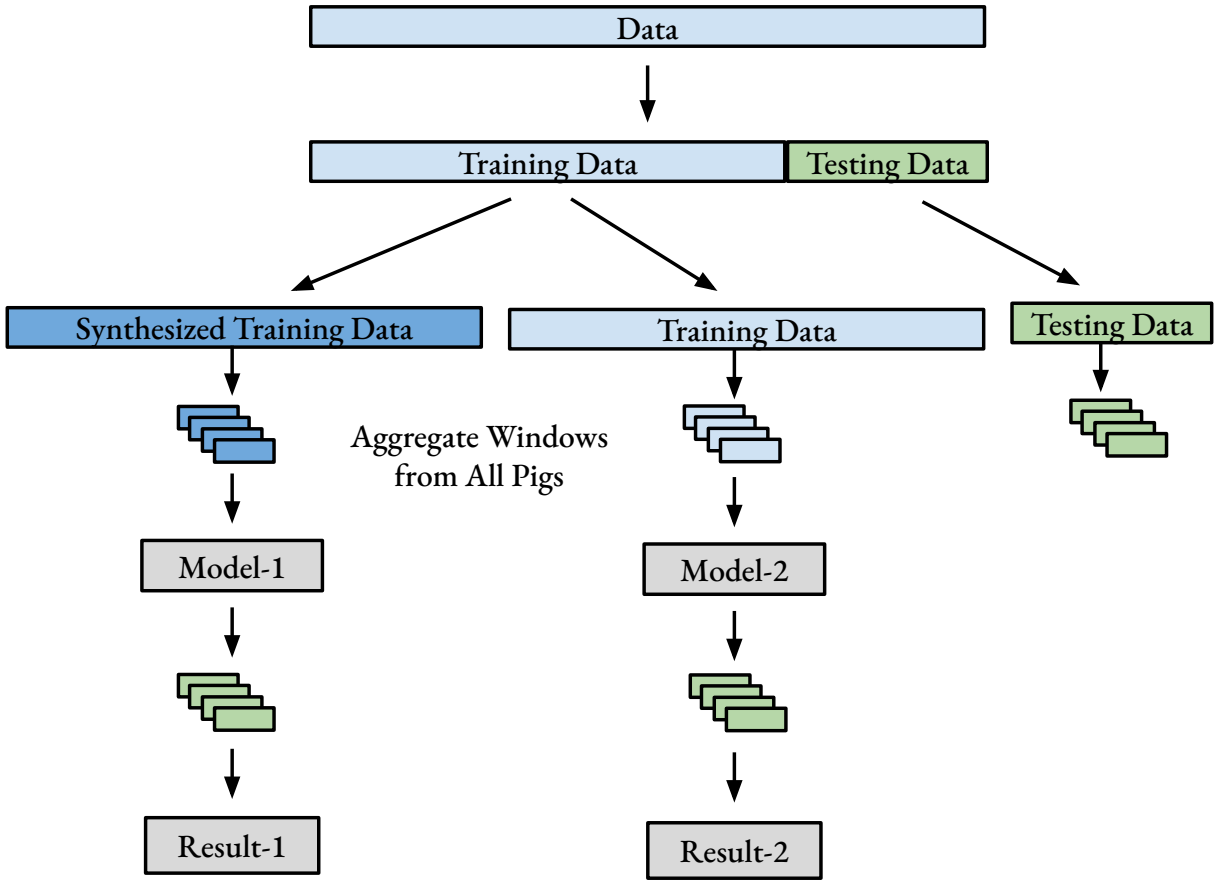

Figure 17: This diagram explains the training and testing procedures. The testing results are reported in Table 7.

MAC and PRO Classification

Table 7: MAC and PRO classification results. (The results obtained by using the experimental data are shown in parenthesis, and those obtained by using the model-synthesized data are shown outside of the parenthesis.)

(a) MAC and PRO classification using PAP data.

-	MAC Estimated	PRO Estimated
MAC	93.33% (90.56%)	6.67% (9.44%)
PRO	8.33% (9.44%)	91.67% (90.56%)
Accuracy	92.50% (90.56%)	

(b) MAC and PRO classification using PVP data.

-	MAC Estimated	PRO Estimated
MAC	85.56% (98.33%)	14.44% (1.67%)
PRO	14.72% (9.44%)	85.28% (90.56%)
Accuracy	85.42% (94.44%)	

Proposed Signal Model on CHARIS Dataset

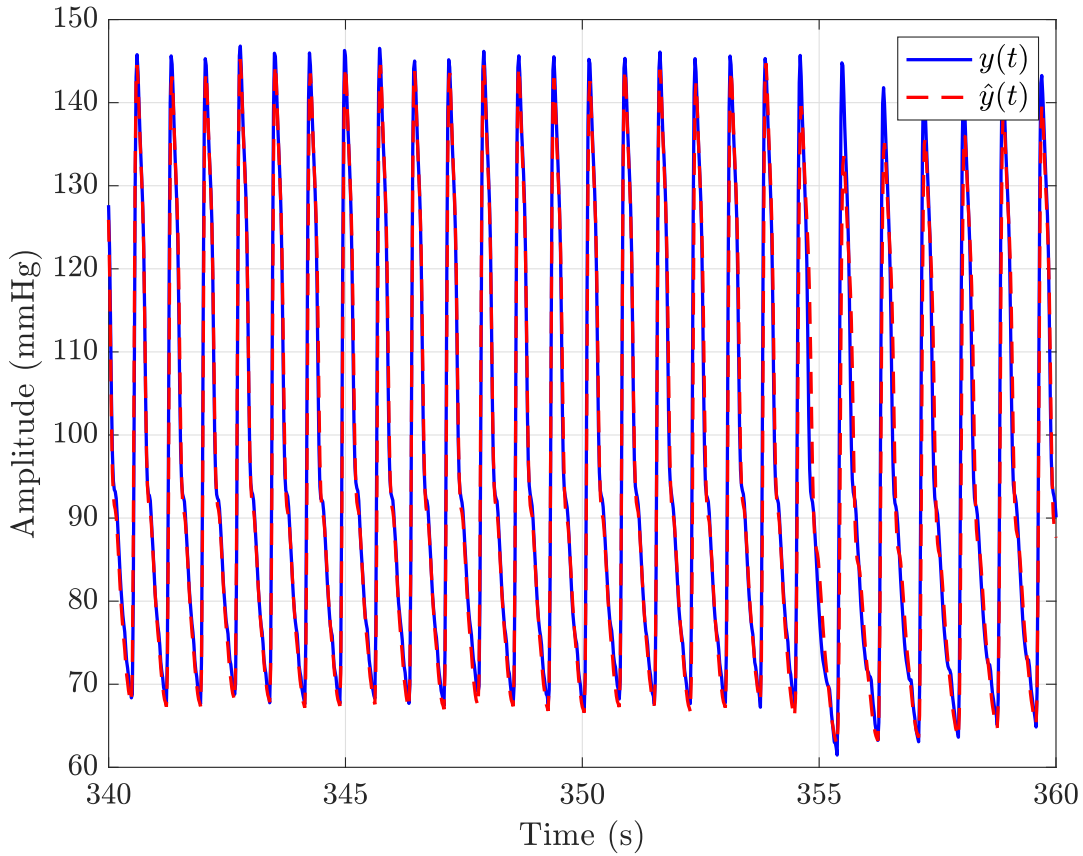

Figure 18: Comparison of arterial pressure signal $y(t)$ and corresponding model fit $\hat{y}(t)$ from subject 10 of the CHARIS [KKK+16] dataset. This 15-minute data fit has $\rho = 0.990$.

Proposed Signal Model on CHARIS Dataset

Table 8: Correlation coefficient ρ for the IPFM model in CHARIS data with human subjects.

Subject	ρ	Subject	ρ	Subject	ρ
1	0.959	6	0.989	11	0.978
2	0.960	7	0.992	12	0.974
3	0.988	8	0.990	13	0.989
4	0.964	9	0.988	-	-
5	0.983	10	0.990	-	-

Dicrotic Notch

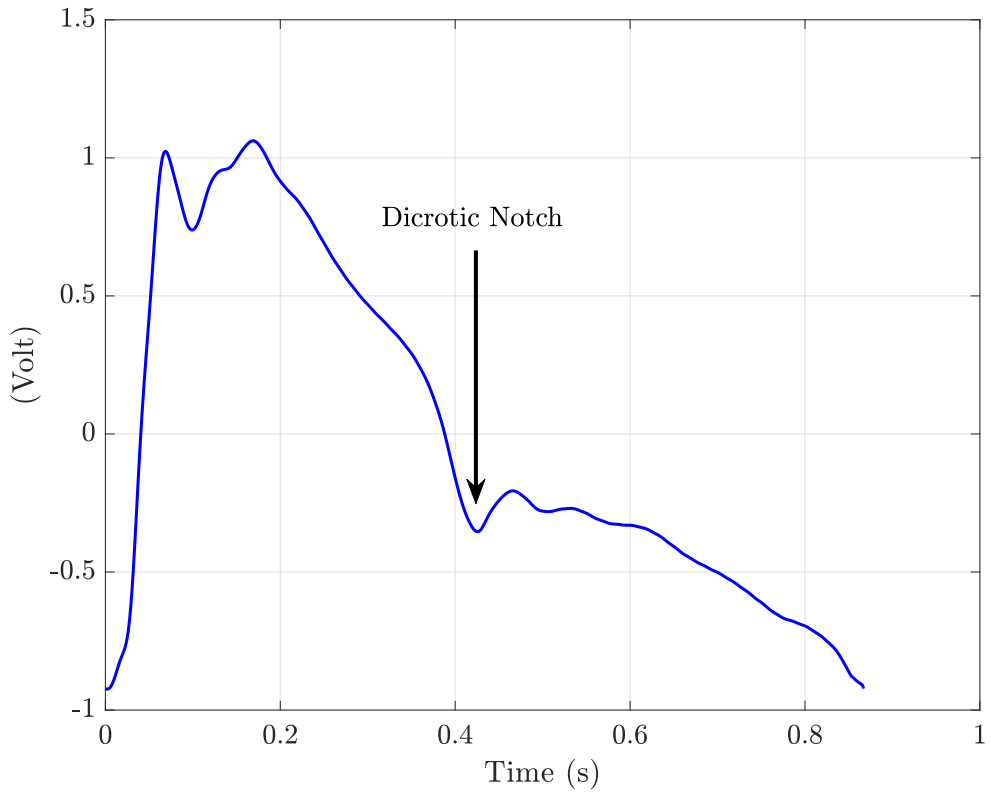

Figure 19: Dicrotic notch in a PAP pulse $p(t)$ in Pig-2 MAC-2. This notch marks the end of systole and the beginning of diastole.

Unit Pulse Shapes

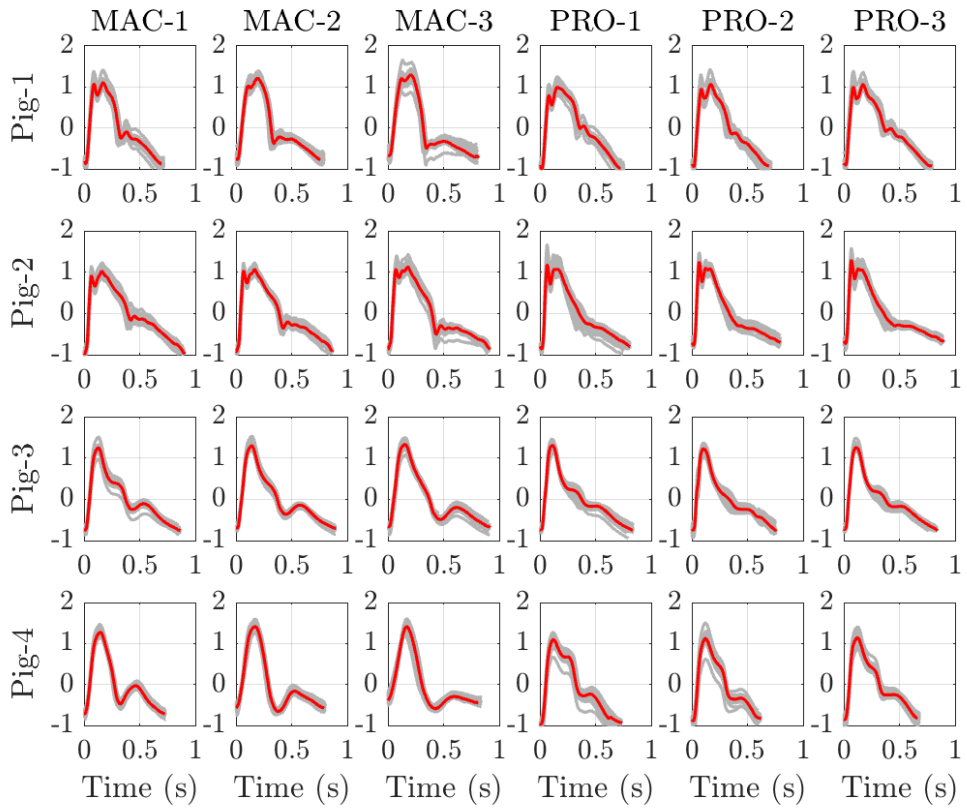

Figure 20: Pulse shapes in PAP signals at the different anesthetic stages. The red pulses are the aggregate averages of gray pulses.

Unit Pulse Shapes

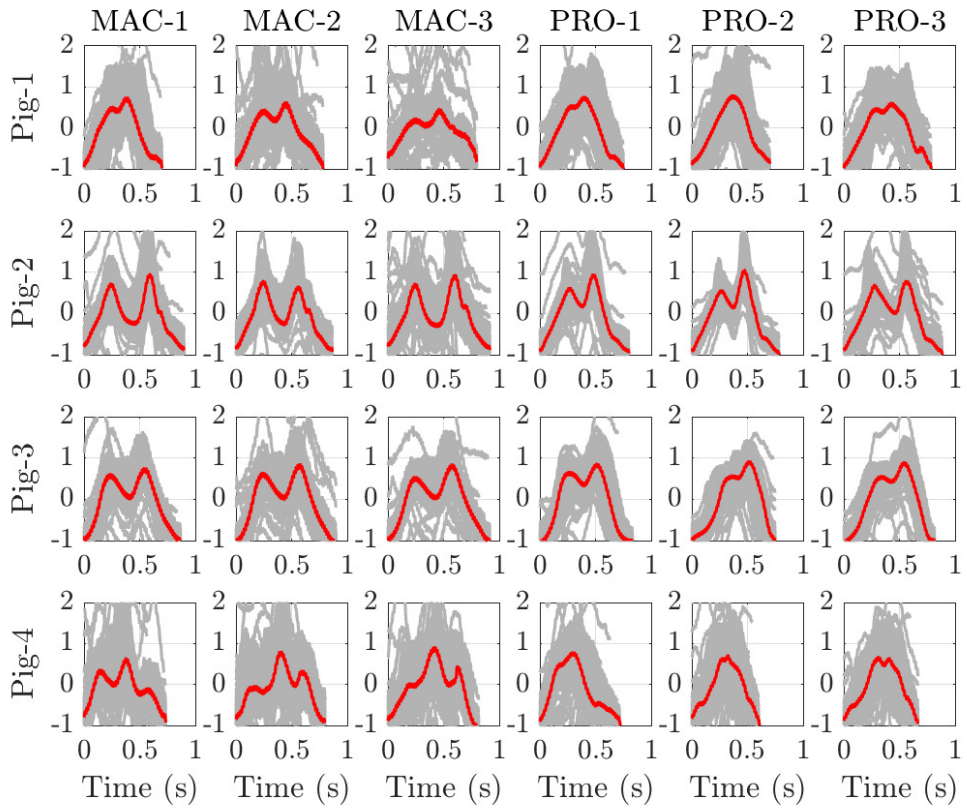

Figure 21: Pulse shapes in PVP signals at the different anesthetic stages. The red pulses are the aggregate averages of gray pulses.

Variation in Pulse Duration

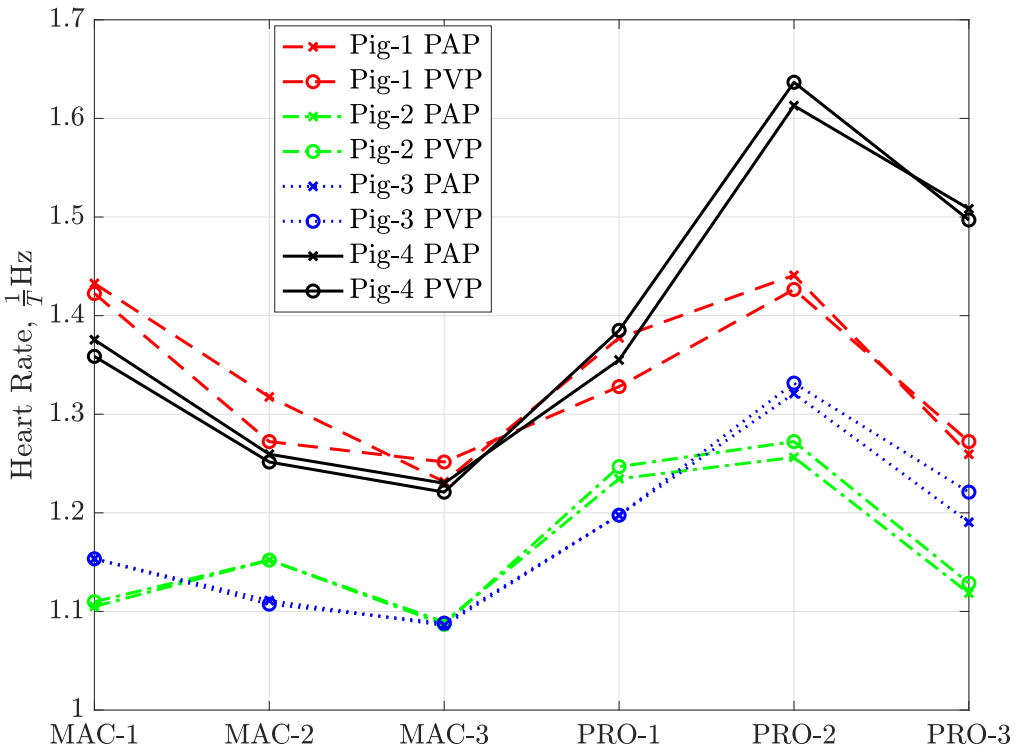

Figure 22: Change in pulse duration (T) of $\hat{y}(t)$ under different levels of Isoflurane and Propofol based on PAP, and PVP signals.

Correlation Between Respiratory and Modulating Signals

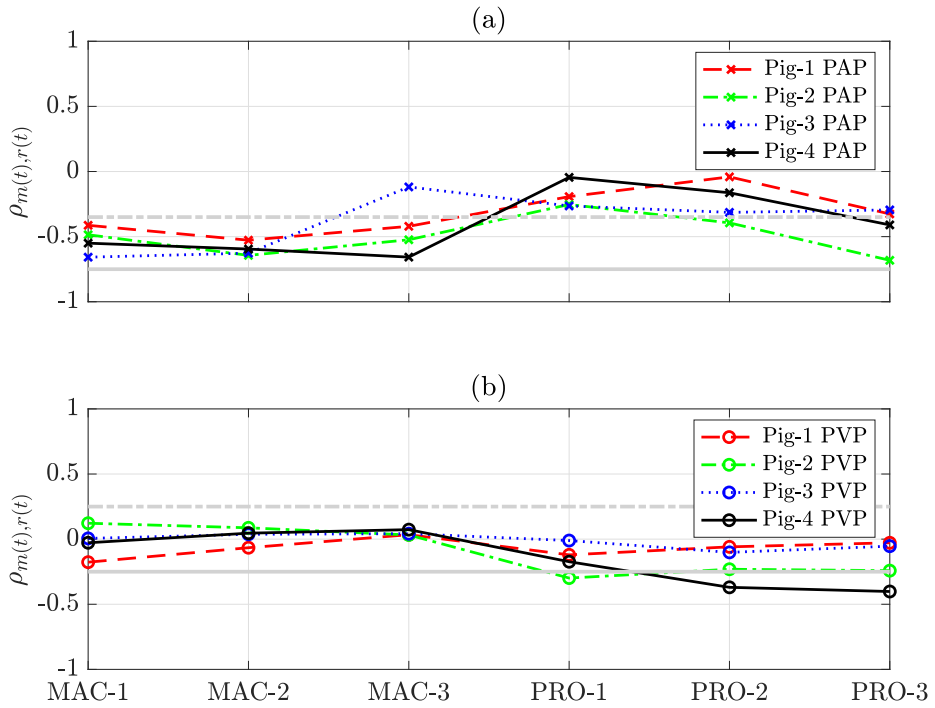

Figure 23: Correlation coefficients of different states between $m(t)$ and $r(t)$ signals. Panels (a) and (b) are based on PAP and PVP signals respectively. The gray horizontal lines in (a) represent $\rho = -0.35$ and $\rho = -0.75$ respectively. Similarly, in (b) the gray lines represent $\rho = 0.25$ and $\rho = -0.25$ respectively.

Outline

Future Works

- Apart from PVP signals, a careful design of experiment should also include ECG, PPG, breathing rate and other related signals
- Side-by-side comparison of PVP and PPG in predicting dehydration or other similar open-ended problems
- The ultimate goal of any long-term future work should include creation of a massive dataset from hydrated and dehydrated subjects under different circumstances
- In ideal scenario, the dataset should be open and available

Outline

List of Publications (First Author Journals)

- **M. A. Hayat**, Jingxian Wu, et al. "Unsupervised Bayesian learning for rice panicle segmentation with UAV images." *Plant methods*, 16.1 (2020): 1-13.
- ✓ **M. A. Hayat**, Jingxian Wu, et al. "Unsupervised anomaly detection in peripheral venous pressure signals with hidden Markov models." *Biomedical Signal Processing and Control*, 62 (2020): 102126.
- **M. A. Hayat**, George Stein, et al. "Self-supervised representation learning for astronomical images." *The Astrophysical Journal Letters*, 911.2 (2021): L33.
- ✓ **M. A. Hayat**, Jingxian Wu, et al. "Modeling Peripheral Arterial and Venous Pressure Signals with Integral Pulse Frequency Modulation," *Biomedical Signal Processing & Control*. [Under Review]

List of Publications

- ✓ P. C. Bonasso, K. W. Sexton, **M. A. Hayat**, et al. "Venous physiology predicts dehydration in the pediatric population." *Journal of Surgical Research*, 238 (2019): 232-239.
- P. C. Bonasso, K. W. Sexton, S. C. Mehl, M. S. Golinko, **M. A. Hayat**, et al. "Lessons learned measuring peripheral venous pressure waveforms in an anesthetized pediatric population." *Biomedical Physics & Engineering Express* 5.3 (2019): 035020.
- A. Z. Al-Alawi, K. R. Henry, L. D. Crimmins, P. C. Bonasso, **M. A. Hayat**, et al. "Anesthetics affect peripheral venous pressure waveforms and the cross-talk with arterial pressure." *Journal of clinical monitoring and computing* 36.1 (2022): 147-159.
- L. D. Crimmins-Pierce, G. P. Bonvillain, K. R. Henry, **M. A. Hayat**, et al. "Critical Information from High Fidelity Arterial and Venous Pressure Waveforms During Anesthesia and Hemorrhage." *Cardiovascular Engineering and Technology* (2022): 1-13.

Research @UArk

- Developed a supervised Gaussian mixture model based rice panicle segmentation algorithm using Markov chain Monte Carlo method
- Unlike deep learning models, it can work on smaller dataset and images with different sizes

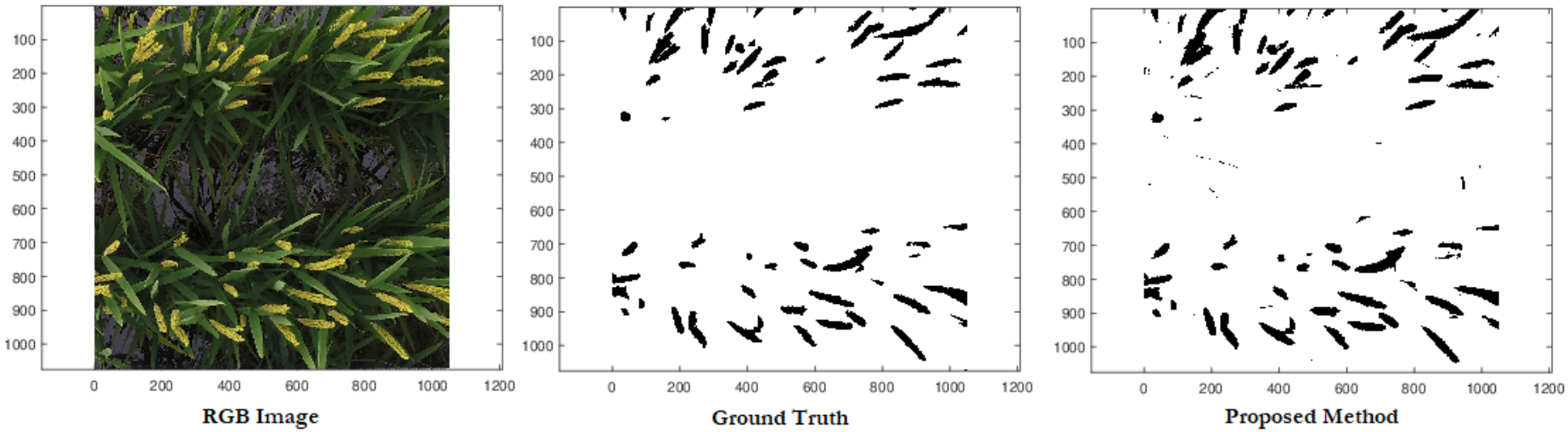

Figure 24: Panicle segmentation

Research @Industry

- Nokia Bell Labs (Summer 2019)
  - OCT image processing using deep learning
- Lawrence Berkeley National Lab (Summer 2020)
  - Self-supervised learning of cosmological image
  - 1 Journal article
  - 1 NeurIPS workshop paper
  - Talk, website and media coverage [link]
- Amazon Web Services - AWS (Summer 2021)
  - Amazon Lookout for Metrics, an anomaly detection service
  - Using forecasting algorithm on anomaly detection

References

[BSM+19] P. C. Bonasso *et al.*, "Lessons learned measuring peripheral venous pressure waveforms in an anesthetized pediatric population," *Biomedical Physics & Engineering Express*, vol. 5, no. 3, p. 035 020, 2019.

[KKK+16] N. Kim *et al.*, "Trending autoregulatory indices during treatment for traumatic brain injury," *Journal of clinical monitoring and computing*, vol. 30, no. 6, pp. 821–831, 2016.

[LS04] P. Laguna and L. Sörnmo, "Modelling heart rate variability," in *Proceedings of the sixteenth international symposium on mathematical theory of networks and systems. Loeven*, 2004, pp. 1–6.

[ML00] J. Mateo and P. Laguna, "Improved heart rate variability signal analysis from the beat occurrence times according to the ipfm model," *IEEE Transactions on Biomedical Engineering*, vol. 47, no. 8, pp. 985–996, 2000.

[WMB04] J. E. Wathen, T. MacKenzie, and J. P. Bothner, "Usefulness of the serum electrolyte panel in the management of pediatric dehydration treated with intravenously administered fluids," *Pediatrics*, vol. 114, no. 5, pp. 1227–1234, 2004.

[ZHMM03] W. Zong, T. Heldt, G. Moody, and R. Mark, "An open-source algorithm to detect onset of arterial blood pressure pulses," in *Computers in Cardiology, 2003*, IEEE, 2003, pp. 259–262.

Outline

Q&A

- Thank you for your patience!
- Questions?
- Feedback/Suggestions?